HYDROGEN PRODUCTION FROM AMMONIA BORANE BY USING PALLADIUM-NICKEL BIMETALLIC NANOPARTICLES SUPPORTED ON SILICA COATED-COBALT FERRITE MAGNETIC NANOPARTICLES

A THESIS SUBMITTED TO

THE GRADUATE SCHOOL OF NATURAL AND APPLIED SCIENCES

OF

ATILIM UNIVERSITY

BY

ABDULMUNEM ABOURAWI MOHAMMED ARAKEZE

IN PARTIAL FULFILLMENT OF THE REQUIREMENTS FOR THE DEGREE OF MASTER OF SCIENCE

IN

APPLIED CHEMISTRY

AT

THE DEPARTMENT OF CHEMICAL ENGINEERING AND APPLIED CHEMISTRY

JULY 2016

Approval of the Graduate School of Natural and Applied Sciences, Atılım University.

_____

Prof. Dr. İbrahim AKMAN

Director

I certify that this thesis satisfies all the requirements as a thesis for the degree of Master of Science.

_____

Prof. Dr. Atilla CİHANER

Head of Department

This is to certify that we have read the thesis "Hydrogen Production from Ammonia Borane by Using Palladium-Nickel Bimetallic Nanoparticles Supported on Silica Coated-Cobalt Ferrite Magnetic Nanoparticles" submitted by "Abdulmunem Abourawi Mohammed Arakeze" and that in our opinion it is fully adequate, in scope and quality, as a thesis for the degree of Master of Science.

_____

Assoc. Prof. Dr. Murat KAYA

Supervisor

Examining Committee Members

Asst. Prof. Dr. Ferdi KARADAŞ _____

Assoc. Prof. Dr. Seha TİRKEŞ _____

Assoc. Prof. Dr. Murat KAYA _____

Date: 13.07.2016

I declare and guarantee that all data, knowledge and information in this document has been obtained, processed and presented in accordance with academic rules and ethical conduct. Based on these rules and conduct, I have fully cited and referenced all material and results that are not original to this work.

Name, Last name: Abdulmunem Abourawi Mohammed Arakeze

Signature:

ABSTRACT

HYDROGEN PRODUCTION FROM AMMONIA BORANE BY USING PALLADIUM-NICKEL BIMETALLIC NANOPARTICLES SUPPORTED ON SILICA COATED-COBALT FERRITE MAGNETIC NANOPARTICLES

ARAKEZE, Abdulmunem Abourawi Mohammed
M.Sc., Chemical Engineering and Applied Chemistry
Supervisor: Assoc. Prof. Dr. Murat KAYA
July 2016, 42 pages

Due to their high activity in catalytic systems nowadays metal nanoparticles have attracted much attention. They have known as quasihomogeneous system which bridging homogenous and heterogeneous catalysis. Metal nanoparticles have high surface energy so they are not stable form larger particles in catalytic processes. Besides separation of metal nanoparticles are not easy from the reaction media. To separate them, filtration and centrifugation processes are applied. In order to get rid of the disadvantages of naked nanoparticles and to enhance the stability and to obtain reusable catalysts, immobilization of nanoparticles onto inorganic support materials are necessary.

In this thesis, novel catalyst contains of palladium-nickel bimetallic nanoparticles supported on silica coated magnetic particles has been prepared. After addition of Pd^{2+} and Ni^{2+} ions on silica coated cobalt ferrite magnetic support, bimetallic nanoparticles formed by reduction of the Pd^{2+} and Ni^{2+} ions with NH_3BH_3 on the surface of silica coated magnetic support materials.

The characterization of nanocomposite catalysts were done by inductively coupled plasma/optical emission spectrometry (ICP-OES), X-ray diffraction (XRD), X-ray photoelectron spectroscopy (XPS), transmission electron microscopy (TEM), high resolution- transmission electron microscopy (HR-TEM) and N_2 adsorption–desorption technique. Palladium-Nickel bimetallic nanoparticles supported on silica coated cobalt ferrite (PdNiNPs/SiO_2-$CoFe_2O_4$) provide an initial turnover frequency (TOF) of 197 min^{-1} at room temperature. Another important advantage of such catalyst system is that, catalysts can be collected with an external magnet in the reactor wall and they can be reused without losing activity and sample lost.

Keywords: Metal nanocatalyst, hydrogen energy, magnetic separation, ammonia borane, dehydrogenation

ÖZ

SİLİKA KAPLI KOBALT FERRİT MANYETİK PARÇACIKLAR ÜZERİNE TUTTURULMUŞ BİMETALİK PALADYUM-NİKEL NANOPARÇACIKLARIN KULLANIMI İLE AMİN BORANDAN HİDROJEN ÜRETİLMESİ

ARAKEZE, Abdulmunem Abourawi Mohammed
Yüksek Lisans, Kimya Mühendisliği ve Uygulamalı Kimya Bölümü
Tez Yöneticisi: Doç. Dr. Murat KAYA
Temmuz 2016, 42 sayfa

Günümüzde katalitik sistenlerdeki yüksek aktiflikleri sebebi ile metal nanoparçacıklar ilgi çekmektedir. Metal nanoparçacıklardan hazırlanan katalizörler homojen ve heterojen katalizörler arasında bir köprü olarak bilinirler. Metal nanoparçacıklar sahip oldukları yüksek yüzey enerjileri sebebi ile sabit değillerdir ve katalitik uygulamalarda birleşerek büyük parçacıklar oluşturma eğilimindedirler. Bunun yanında bu nanoparçacıkları reksiyon ortamından uzaklaştırmak çok zordur. Bunları ayırmak için filtreleme ve santrifuj işlemleri uygulanmaktadır. Sadece metal nanoparçacıkların kullanımından doğan dezavantajları ortadan kaldırmak ve kararlılığı arttırmak ve tekrar kullanımı olan katalizörler elde edebilmek için nanoparçacıkların inorganik destek malzemeleri üzerine sabitlenmesi gerekmektedir.

Bu tezde, silika kaplı manyetik parçacıklar üstünde desteklenmiş paladyum ve nikel bimetalik nanoparçacıklarını içeren yeni bir katalizör sistemi hazırlanmıştır. Pd^{2+} ve Ni^{2+} iyonlarının silika kaplı kobalt ferrit nanoparçacıklarına eklenmesinden sonra, NH_3BH_3 ile birlikte Pd^{2+} ve Ni^{2+} iyonlarının silika kaplı manyetik nanoparçacıkların yüzeyinde indirgenmesi sonucunda istenilen bimetalik nanoparçacıklar elde edilmiştir.

Nanokompozit katalizörlerin karakterizasyonu indüktif olarak eşleşmiş plazma optik emisyon spektrometresi (ICP-OES), X-ışını kırınımı (XRD), X-ışını fotoelektron spektroskopisi (XPS), geçirimli elektron mikroskobu (TEM), yüksek çözünürlüklü- geçirimli elektron mikroskobu (HR-TEM) ve N_2 adsorpsiyon–desorpsiyon teknikleri ile yapılmıştır. Silika kaplı kobalt ferrit ($PdNiNPs/SiO_2$-$CoFe_2O_4$) parçacıkları üstünde desteklenen paladyum-bakır bimetalik nanoparçacıkları, oda sıcaklığında, başlangıçta 197 dk^{-1}'lik çevrim frekansı sağlamıştır. Bu katalizör sistemlerinin bir diğer önemli avantajı ise, katalizörün harici bir mıknatıs yardımıyla reaktör duvarında toplanabilmesi ve sürdürülebilir katalitik aktivite özelliği sayesinde tekrar kullanılabilmesidir.

Anahtar Kelimeler: Metal nanokatalizör, hidrojen enerjisi, manyetik ayırma, amin boran, de-hidrojenlenme

This work has been carried out for the sake of Allah and in order to attain his mercy and pleasure

ACKNOWLEDGEMENTS

In the name of Allah first and foremost, all praise be due to Allah, the almighty, for giving me the ability, health and knowledge to complete this work, for without him, I would not have been able to start, let alone to finish it.

I would like to express my deepest appreciation to my supervisor Assoc. Prof. Dr. Murat Kaya for his support, guidance, encouragement and patience during my research. He was not only my supervisor but also my friends in my life. I owe great thanks to him.

I owe an enormous debt to my parents whom have been a constant source of support and encouragement during my life**.**

I gratefully thank to my wife and my love Naden for everything, she gave especially her kindness, love, patience and her immense support all the way through my master studies. And also to my lovely child Abdalmuhiman who has decorated my life and made it full of happiness and joy.

I would also like to thank to my brothers and sisters for their encouragement and support. And also I wish to express my thanks to my lovely home country Libya.

I am also grateful to the Canan Karabay and Ceren Uzun for their support, guidance and encouragement during my master study. Also, I wish to express my thanks to all academic staffs in the Department of Chemical Engineering and Applied Chemistry at Atilim University for their efforts and helps.

TABLE OF CONTENTS

LIST OF FIGURES

FIGURES

LIST OF TABLES

TABLE

LIST OF ABBREVIATIONS

AB	-	Ammonia Borane
APTMS	-	(3- aminopropyl) trimethoxysilane
BET	-	Brunauer- Emmett- Teller
BJH	-	Barret-Joyner-Halenda
E_a	-	Activation Energy
EDX	-	Energy Dispersive X-ray
FE-SEM	-	Field Emission Scanning Electron Microscopy
H_c	-	Coercivity
H_{sat}	-	Saturation Field
HR-TEM	-	High Resolution Transmission Electron Microscopy
ICP-OES	-	Inductively Couple Plasma- Optical Emission Spectroscopy
M_r	-	Remanent Magnetization
M_s	-	Saturate Magnetization
MSC	-	Magnetically Separable Catalyst
TEOS	-	Tetraethyl Orthosilicate
TOF	-	Turnover Frequency
TON	-	Turnover Number
TTON	-	Total Turnover Number
XRD	-	X-ray Diffraction

CHAPTER 1

INTRODUCTION

Hydrogen as the cleanest and non-polluting energy source can satisfy continous transition from fossil fuels to renewable energy sources.[1] To obtain efficient storage and hydrogen production, convenient and sufficient hydrogen storage and releasing materials are under great consideration. Accordingly, with its low molecular weight (30.9 g/mol), inert nature towards full cell applications, nontoxic character, higher hydrogen density (19.6 wt %) and the content (9 wt %), ammonia-borane (NH_3BH_3, AB) is the target of 2015 U.S. Department of Energy.[2,3]

Thermal decomposition in solid state[4] and dehydrocoupling/dehydrogenation[5] in organic solvent are the methods that promote hydrogen release from AB, however, throughout the transition metal catalyzed hydrolytic dehydrogenation of AB, much more hydrogen formation can be observed due to rapid hydrogen production in spite of moderate conditions.[6] It was known that nearly 3 equivalence of hydrogen per mole of AB can be produced by using aqueous solution of AB via a metal catalyst at room temperature.

There are several researches in literature that can be used as homogenous[7] and heterogeneous[8] catalysts for the hydrolytic dehydrogenation of AB. Despite the proper homogenous catalysts for hydrolytic dehydrogenation[7], recently, because of simple separation and catalyst recovery properties, heterogeneous catalyst has become more popular. Ru,[9] Rh,[10] Pd,[11] Pt,[12] and Au[13] are the noble metals that exhibit high catalytic activity in the hydrolytic dehydrogenation of AB, yet these

metals are not practical so that there is high tendency towards the enhancement of low cost catalyst systems for this important reaction.

Nowadays, 3d transition metals such as Fe,[14] Co,[15] Ni[16], and Cu[17] have gained importance for applying as catalyst in the reaction of hydrolytic dehydrogenation of AB. On the other hand, these metals exhibit low activity and reusability performance. For this reason, the enhancement of metal catalyst that exhibit high activity, catalyst recovery and reuse property besides low cost is crucial for this important reaction.

In order to decrease the cost and to increase the activity, recently, the usage of non-precious metals such as Co, Ni, Fe, or Cu with precious metals to obtain bimetallic nanoparticles (Au-Ni, Pt-Co) gained great importance. Furthermore, these catalysts can be isolated easily and have reusable property so that they show suitable recovery and catalyst recycling for continuous chemical processes.

1.1 Hydrogen Energy

Today, although there are several harmful effects of fossil fuels on ecology and environment, nearly 80 % of the energy supply is acquired from fossil fuels.[18] Recently, consuming of reserves and raw materials and besides the impact of air pollution and change on climate and human health are crucial topics. CO_2 is one of the greenhouse gases that are released through the combustion of fossil fuels that is followed with great interest. Alternatively, effective and new technologies and different energy investments such as solar, wind, hydropower energy is suggested as energy sources to eliminate the problems about negative environmental effects and security throughout the usage of fuel. These renewable energy sources, on the other hand, have some disadvantages such as having continuity problems (presence of available solar and wind energy) and the high cost. The unpleasant outcome of this event can be prevented via energy storage. In this regard, hydrogen as renewable energy source is additionally safe, plenty, and clean. There are several sources for obtaining hydrogen and it can combine with oxygen to form water, and the reaction with carbon, nitrogen and oxygen is taking place in living things and with fossil fuels.[19]

The separation of hydrogen from other elements forms molecular hydrogen (H_2), an environmental friendly fuel that reacts with oxygen to form only water.[19] The problems arising from the usage of hydrogen should be removed if it is desired to utilize as energy carrier. In order to realize hydrogen economy, four main conditions should be achieved mentioned below:[20]

- Production – Enhancement of production methods that expend low amount of energy to generate hydrogen and renewable fabrication of large amount of hydrogen.
- Storage – Simple storage and transport capacity to become easily proper energy source.
- Power generation – Effective power production system that spends hydrogen for portable applications.
- Safety –Particular preventions and measurements should be made provision against flammability of hydrogen throughout usage and storage. Furthermore, reliable methods should be selected to generate and store it.

Although hydrogen has some disadvantages about the production, storage and usage, it is the most significant renewable source for future, yet, it should also be stated that the achievement of recommended systems can be specified by its efficiency. As a part of hydrogen cycle, the important parameters are the cost related with financial and resource, constancy of the reaction and safety that shows the performance and failure of the recommended system to utilize.**Error! Bookmark not defined.**

1.2 Hydrogen Storage Materials

The storage of hydrogen systems have the disadvantages of having low volumetric capacity and safety for portable utilization because of high pressure and cryogenic storage.[21] In this regard, metal hydrides[22], metal organic frameworks[23], nanostructures[24], and chemical compounds[25] are the solid materials that have been

stated in literature as storage material. Therein, chemical compounds(Figure 1.1) have gained great importance because of their high storage capacity, and for this, these substances are proper to be used for fuel cell utilization under environmental conditions.

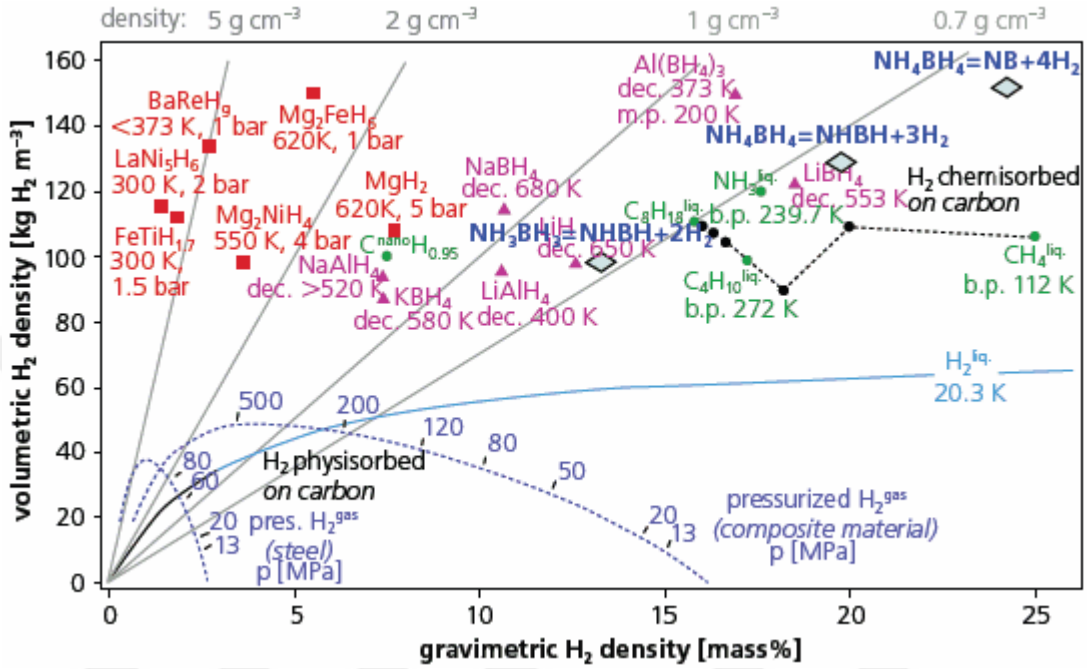

Figure 1.1 Comparison of gravimetric and volumetric densities of various hydrogen storage materials.[26]

1.3 Ammonia Borane

Ammonia borane (AB) adduct is taken into account that it is one of most considerable complex as boron hydride complex for mobile utilizations because it contains high amount of hydrogen; alternatively it is nontoxic and highly stable.[27] AB has a tetragonal crystal structure at room temperature, and besides it has white color with melting point larger than 110 ^{o}C.

The stored hydrogen can be released from adduct via pyrolysis and solvolysis methods. Alternatively, thermal decomposition method at 385 K provides the release of hydrogen with the amount of 6.5 wt % of the initial mass of AB. The increment in the amount of hydrogen release can be provided at temperatures, higher than 500 ^{o}C.[28] Yet, above the temperature of 125 °C, the generation of

volatile unwanted products such as borazine, cycloborazanes, polyaminoborane, and ammonia can pollute the fuel cell.[29]

These are the reasons to achieve catalytic hydrolysis of AB in order to acquire hydrogen practically and effectively at room temperature via using suitable catalyst according to given equation (Eq. 1.1).[30]

$$\mathbf{H_3NBH_{3(aq)} + 2H_2O_{(L)} \xrightarrow{catalyst} NH_4BO_{2(aq)} + 3H_{2(g)}} \quad \text{(Eq. 1. 1)}$$

1.4 What is Catalysis

A catalyst is a substance that increases the rate of reaction without being consumed at the end of the reaction. Alternative mechanism is taking place with distinct transition state via the utilization of a catalyst, and as it increases the reaction, it also results in the decrease of activation energy called as a transition-state theory. With respect to this theory, the entropy of catalyzed reaction during activation is lower than the reaction when the catalyst is utilized. The reason of it is that transition state is immobilized at the surface of catalyst with the following loss of translational freedom. Because of this, according to theory, when the catalyst is used the activation energy of this reaction should be lower than that of the uncatalyzed reaction (Figure 1.2), as a consequence, due to the formation of more molecular collisions, the energy required increases to reach the transition state. The utilization of catalyst in a reaction does not change the extent; that is, due to equal effect of catalyst on both rate of forward and reverse reaction, equilibrium constant stays constant.

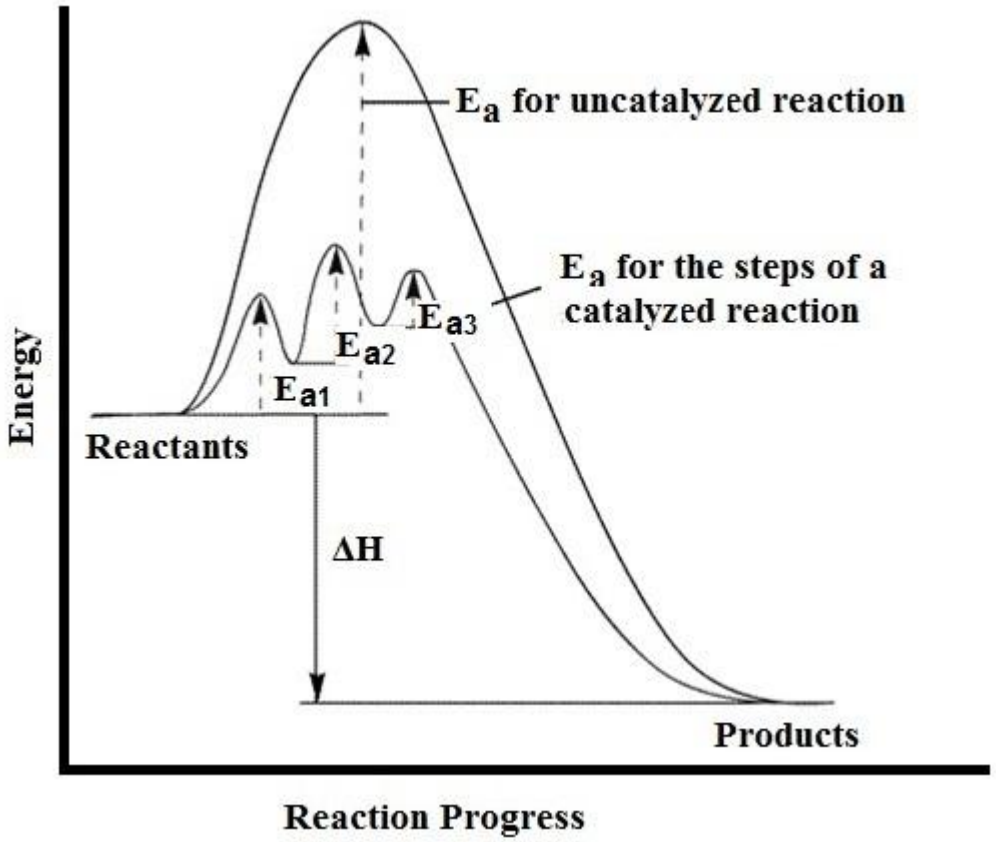

Figure 1.2 Potential energy diagram for an exothermic reaction under both catalyzed and uncatalyzed conditions.[30]

Despite the distinct type of catalysts such as Lewis acids, organometallic complexes, polymers, enzymes and so on, the fundamental categories are heterogeneous catalysts, homogeneous catalyst and biocatalysts. [30]

Homogenous and heterogeneous catalyst can be categorized depending on being distinct or same phase with reactants during the operation of catalyst. When the catalyst has same phase with reactants and products, called as homogenous catalysis, and this type of catalyst, contains transition metal and stabilization of the catalyst is provided by a ligand attaching to the central atom. Here, the properties of catalyst depend on the ligands that are used. Conversely, in heterogeneous catalysis, the catalyst and reactants have distinct phases. In this kind, the reactants diffuse to the metal catalyst surface and by chemisorptions, adsorption onto surface occurs.[30]

After the reaction is finished, products are released and removal of them is taking place from the surface. In heterogeneous type catalyst, the presence of catalytic sites belongs to surface area of it. Recently, in distinct areas of chemical and energy industries, heterogeneous catalysts have become popular. In nature, there are several catalytic processes that can be examples of heterogeneous catalyst that include a catalyst in solid phase and reactants in gas or liquid phase. Today's, easy separation reusability, stability, low-cost and low-toxicity are the crucial factors that make these catalysts to be preferred in the processes of industry.[30]

1.5 Importance of Magnetic Nanoparticles

The properties of magnetic nanoparticles are dramatically distinct from their bulk counterparts, and nowadays due to their important properties, they can be used in several applications[31] such as biotechnology, magnetic fluids, magnetic resonance imaging, data storage, environmental remediation, and catalysis.[32]

Magnetic properties of them can be altered by changing the dimensions, shape, composition and crystal structure of nanomaterials. Yet, it is not so easy to maintain the same property with the same type of nanoparticles in spite of having approximately same chemical composition and size throughout the synthetic period.[33]

1.6 Production of Magnetic Nanoparticles

In order to synthesize nanoparticles, there are several synthetic routes that include gas, liquid or solid phase production. Generally, it was mentioned in literature that thermal decomposition, micro emulsion, hydrothermal and solvothermal techniques, sonochemical, polyol, and co-precipitation techniques are the suitable techniques in order to produce nanoparticles with different compositions and phases.[34]

Co-precipitation is an easy and practical technique for the synthesis of magnetic nanoparticles from aqueous solutions of salt precursors with a base as reducing agent at room or elevated temperatures. Type of salts (e.g., chlorides, sulfates, nitrates) used for synthesis, the ratio of the ions, the temperature, pH, ionic strength of the medium are important parameters that affect size, shape, and composition of synthesized nanoparticles. High scale synthesis and simplicity make the method advantageous for the synthesis of magnetic nanoparticles.[34]

1.7 Surface Coating of Magnetic Nanoparticles

The unwanted interactions between magnetic core and catalyst that is bonded to surface should be prevented via a strong barrier. These undesirable interactions between catalyst and core and agglomeration of synthesized nanoparticles can be prevented by silica layer. Furthermore, silica coating provides through silanol groups on surface, modification and addition of nanoparticle to surface with ease.[35]

Sol-gel technique is one of the wet-chemical methods that are utilized for silica coating on nanoparticles. The technique is related with Stöber method that the surface coverage of particles is supplied via silica layer[36] through hydrolysis reaction and subsequent condensation reaction of an alkoxide. Mostly tetraethyl orthosilicate (TEOS) in alcohol- water mixtures is utilized as a silicon precursor that is catalyzed by a base.

The thickness of silica layer depends on the reaction conditions. In the literature, it is stated that as the amount of TEOS in water, isopropanol and ammonia (30 % v/v) solution containing magnetic fluid changes, the thickness of silica layer around nanoparticles can be controlled.[37] As the thickness of silica shell (2-100 nm size range) on magnetic nanoparticle is controlled, at the same time, the inhibition of homogenous nucleation of silica nanoparticles should be achieved.

1.8 Magnetically Recoverable Nanocatalysts

Green chemistry, also called as a sustainable chemistry, is a science that designs chemical products and methods to provide minimum utilization and formation of deleterious substances. Green catalysis is one of the most important topics of green chemistry. Nowadays, researchers are interested in the enhancement of sustainable and eco-friendly synthesis procedures to inhibit the utilization of dangerous organic solvent, unhealthy chemicals, hazardous and vigorous reaction requirements and in achievement of the easy, time-saving and effective separation throughout the process.[38]

Despite the broad usage of catalysts in industry, isolation and removal of the final product after the reaction finishes are the most important problems of them. This case results in the inappropriate process. In very low amount of catalyst that is at ppm or ppb level can be found in the product although it is removed from the reaction medium. Separation of catalyst is required to inhibit contaminations arising from metals in drug and pharmaceutical products. For this, heterogeneous catalyst provides the isolation and separation of catalyst from reaction medium readily.[39] In heterogeneous catalytic systems, the active molecules can bind onto the surfaces or immerse inside through the porous structure of silica, alumina or ceria supports by entrapment or embedding methods.

Grafting is achieved through the covalent binding or physical adsorption of the catalyst. However, the access of active sites for heterogeneous catalyst is difficult compared to homogenous catalysts, and this event results in the reduction of catalyst activity. Therefore, a catalytic system should carry both high activity and selectivity property of homogenous system, and the separation and recovery property of heterogeneous catalyst simultaneously. All these wanted properties can be obtained via nanocatalysis systems. The superiority of both heterogeneous and homogenous catalysis systems can be gathered with nanocatalyst, and supply the wanted properties of both systems.

Although the nanocatalysts have several benefits compared to other catalyst systems, it shows the disadvantages of adversity in isolation and recovery after reaction is completed. The conventional methods such as filtration and centrifugation are not suitable because of the small size of the nanocatalyst and this results in the difficulty of utilization of nanocatalyst economically.

In order to remove this problem, magnetic nanoparticles can be utilized in nanocatalyst systems. These particles are insoluble and as they exhibit paramagnetic property, they can remove from the reaction system with ease via an external magnetic field. These sufficient qualities provide the magnetic nanoparticles as pleasant materials with extension interest.[40] Magnetically separable catalysts (MSC), additionally, suggest important efficiency in a broad range of reactions because of the probability of surface functionality through the preparation of catalyst.

1.9 Aim of the Study

In this study, SiO_2-$CoFe_2O_4$ nanocomposite material was used as a support material for palladium-nickel bimetallic nanoparticles (Pd(0)Ni(0)/SiO_2-$CoFe_2O_4$). In order to prepare Pd(0)Ni(0)/SiO_2-$CoFe_2O_4$ magnetic material, Pd(II) and Ni(II) ions were added by using wet-impregnation of on SiO_2-$CoFe_2O_4$ followed by *in-situ* reduction of the ions with NH_3BH_3 on the surface of magnetic SiO_2-$CoFe_2O_4$ particles. The prepared materials were characterized by using ICP-OES, XRD, SEM, TEM, HR-TEM, EDX and N_2 adsorption–desorption technique. Then the prepared catalyst was used in the hydrogen production from aqueous solution of ammonia-borane at room temperature. The reusability of the prepared catalyst was also investigated.

CHAPTER 2

MATERIALS AND METHODS

2.1. Materials

In this study, palladium(II) nitrate ($Pd(NO_3)_2 \cdot xH_2O$), nickel(II)chloride, ($NiCl_2$), iron(III) chloride hexa-hydrate ($FeCl_3.6H_2O$), cobalt (II) chloride hexa-hydrate, ($CoCl_2.6H_2O$), ammonia-borane (NH_3BH_3), tetraethylorthosilicate (TEOS), (3-Aminopropyl)trimethoxysilane (APTMS), ammonium hydroxide (NH_4OH), sodium chloride (NaCl) and sodium hydroxide (NaOH), were purchased from Sigma-Aldrich in analytical grades and used as received. Milli-Q Water Purification System was used to obtain deionized water. Washing of glassware was done with ethanol and water.

2.2. Characterization

Perkin Elmer inductively coupled plasma optical emission spectroscopy (ICP-OES) was used to figure out the nickel and palladium content of the catalyst (loaded onto the silica coated cobalt ferrite (SiO_2-$CoFe_2O_4$) magnetic support). Leaching of loaded metals after the reaction was also monitored by using ICP-OES.

The crystal structure of the catalyst was investigated by using Rigaku Ultima-IV model X-ray diffraction (XRD) spectrometer. XRD patterns of prepared and used particles were obtained in the range of 2θ = 5- 60º.

The morphological characterization of the prepared particles were investigated by using QUANTA 400F Field Emission Scanning Electron Microscope (FE-SEM), JEOL JEM-2010F (FEG, 80-200 kV) transmission electron microscopy (TEM) and high resolution-TEM (HR-TEM). Elemental composition of prepared samples was revealed with energy-dispersive X-ray analyzer (EDX) coupled with SEM and TEM.

ADE Magnetics EV9 Model Vibrating Sample Magnetometer was used at room temperature to obtain saturation magnetization value of the prepared catalyst was measured.

2.3. Preparation of Magnetic Cobalt Ferrite ($CoFe_2O_4$) Nanoparticles as Support Material

Co-precipitation method [34, 41] was used in order to prepare the core part of the magnetic support (Figure 2.1). Initially 25 mL of 0.2 M $CoCl_2.6H_2O$ and 25 mL, 0.4 M $FeCl_3.6H_2O$ aqueous solutions were prepared. Then, 25 mL of 3.0 M NaOH and 12.5 mL of 1.5 M NaCl solutions were prepared separately. After that, 3.0 M NaOH and 1.5 M NaCl solutions were added drop wise slowly into the initially prepared mixture. The final solution was stirred in ultrasonic bath for additional 1 hour at 80 ^oC. At the end of this period, the solution was cooled and the $CoFe_2O_4$ nanoparticles formed were collected by using external magnet and washed with deionized water. Finally the $CoFe_2O_4$ nanoparticles re-dispersed and in de-ionized water and stored at room temperature for further applications.

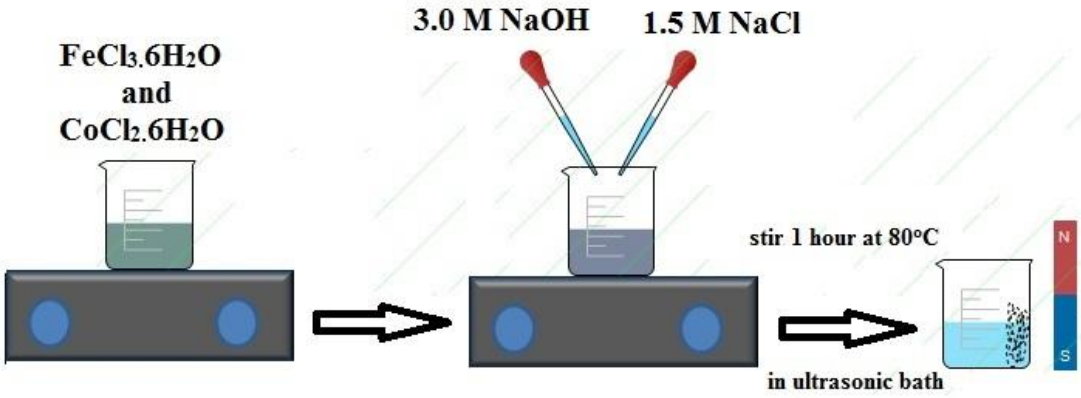

Figure 2.1 Co-precipitation method applied to prepare $CoFe_2O_4$ magnetic nanoparticles.

2.4. Silica Coating of Cobalt Ferrite (SiO_2-$CoFe_2O_4$) Magnetic Nanoparticles

Silica shell over $CoFe_2O_4$ nanoparticles was added by using Stöber method shown in Figure 2.2.[42] According to this method, 80 mL ethanol, 169 µL TEOS and 14.4 µL APTMS were mixed into the beaker. Then, 100 mg $CoFe_2O_4$ nanoparticles was dispersed in 20 mL water and added to the ethanol solution. After that the mixture was stirred for 5 hours at room temperature. Finally silica coated $CoFe_2O_4$ nanoparticles were collected with the help of external magnet and washed with de-ionized water and ethanol. The prepared silica coated $CoFe_2O_4$ nanoparticles were dried and stored.

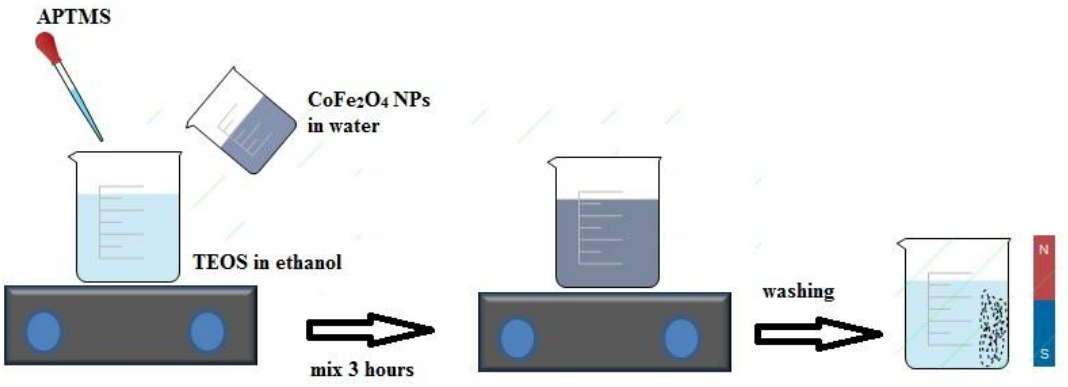

Figure 2.2 Silica coating over $CoFe_2O_4$ magnetic nanoparticles.

2.5. Addition of Pd(II) and Ni(II) Ions on to the Magnetic Support Material

Nickel and palladium ions were added on to the magnetic support (SiO_2-$CoFe_2O_4$) material were prepared by using wet-impregnation method.[41] According to this method, initially 100 mg SiO_2-$CoFe_2O_4$ magnetic nanoparticles was dispersed in 10 mL de-ionized water and then certain amount of $Pd(NO_3)_2.xH_2O$ and $NiCl_2$ added to obtain nickel and palladium ions added magnetic nanoparticles (Pd(II)Ni(II)/SiO_2-$CoFe_2O_4$). Then the mixture was stirred for 5 h at room temperature. At the end of this period, ion added particles were separated by using external magnet and washed time with water. Finally, prepared Pd(II)Ni(II)/SiO_2-$CoFe_2O_4$ particles were dried at 100 ^oC and stored.

2.6. In-Situ Preparation of Palladium-Nickel Nanoparticles Supported on Magnetic Platform (Pd(0)Ni(0)/SiO_2-$CoFe_2O_4$)

Pd(0)Ni(0)/SiO_2-$CoFe_2O_4$ nanoparticles were prepared from the in situ reduction of Pd(II)Ni(II)/SiO_2-$CoFe_2O_4$ nanoparticles during the hydrogen evolution from NH_3BH_3. The activity of the prepared catalysts was figured out by measuring the hydrogen evolution rate in the hydrolysis of ammonia borane (NH_3BH_3).The system used is shown in Figure 2.3. Initially, 10 mg catalyst was dispersed into the reactor by using stirring bar and temperature was regulated to 25.0 ± 0.1 °C by using circulator.

Figure 2.3 System used for the hydrogen production from NH_3BH_3.

In a typical experiment, 10 mL water and 10.0 mg powder of Pd(II)Ni(II)/SiO_2-$CoFe_2O_4$ were added into the reaction vessel thermostated at 25.0 ± 0.1 ºC. Then 100 mM NH_3BH_3 was putted into the reaction vessel. After that the reactor was closed immediately and stirring started.

Pd(0) and Ni(0) nanoparticles were formed initially when ammonia borane added to the mixture. After the formation of metal nanoparticles, hydrogen evolution was started immediately. The evolved hydrogen volume was measured by recording the water level change at every 30 s at a constant temperature and pressure until no more hydrogen evolution was observed.

2.7. Determination of Activation Energy (E_a) for the Reaction Catalyzed by Pd(0)Ni(0)/SiO_2-$CoFe_2O_4$

Activation energy (E_a) of the reaction was revealed by using 10 mg Pd(0)Ni(0)/SiO_2-$CoFe_2O_4$ catalyst at different temperatures (20, 25, 30, 35 ºC). In order to find the optimum amount of catalyst various amounts (10, 15, 20, 25 mg) of Pd(0)Ni(0)/SiO_2-$CoFe_2O_4$ were performed in the hydrolysis of 10 mL of 100 mM (31.8 mg) NH_3BH_3 solution.

2.8. Effect of % Loading of Pd(0)Ni(0) onto SiO_2-$CoFe_2O_4$ Magnetic Support on the Catalytic Activity

Different % loading of Ni(II) and Pd(II) ions were tried in order to find the best performance. 1:1, 1.5:0.5 and 0.5:1.5 Pd/Ni ratios (w/w) were tried and their activity in the hydrogen production from NH_3BH_3were tested by using the method described in the previous section.

2.9. Reuse Performance of the Prepared Catalyst

At the end of the hydrogen evolution from 100 mM NH_3BH_3 by using 10 mg Pd(0)Ni(0)/SiO_2-$CoFe_2O_4$ magnetic nanoparticles at 25 ± 0.1 °C, the nanoparticles was collected to the bottom of the reactor by using an external magnet. After that, the solution part was removed and particles were washed with water before the next run. After washing, nanoparticles were dispersed in 10 mL water and than 1 mmol NH_3BH_3 was added for next run at same temperature. This process was repeated five times and the obtained results were given as the retained catalytic activity with their number of run.

CHAPTER 3

RESULTS AND DISCUSSION

In this study, cobalt ferrite ($CoFe_2O_4$) magnetic nanoparticles were selected as a support material because of the easy preparation method. $CoFe_2O_4$ must be covered to prevent it against the leaching and agglomeration. Besides, silica layer provides the surface for addition of nickel and palladium nanoparticles. After loading the silica coated cobalt ferrite magnetic nanoparticles (SiO_2-$CoFe_2O_4$) with palladium (Pd(II)) and nickel (Ni(II)) ions (Pd(II)Ni(II)/SiO_2-$CoFe_2O_4$), palladium-nickel nanoparticles on silica coated cobalt ferrite magnetic nanoparticles (Pd(0)Ni(0)/SiO_2-$CoFe_2O_4$) were *in situ* generated during the hydrogen production from NH_3BH_3 as a novel catalytic material.

Morphological and magnetic properties, surface area, crystal structure of the SiO_2-$CoFe_2O_4$ magnetic supports were investigated. Then, morphological property, stability, catalytic activity, and reusability of the Pd(0)Ni(0)/SiO_2-$CoFe_2O_4$ nanostructures were revealed.

3.1. Preparation of Magnetic Cobalt Ferrite ($CoFe_2O_4$) Nanoparticles as Support Material

In order to prepare magnetic support material, cobalt ferrite ($CoFe_2O_4$) nanoparticles, modified co-precipitation method were applied. According to this method, highly dispersive small sized $CoFe_2O_4$ magnetic nanoparticles and their agglomerates were synthesized by using $CoCl_2.6H_2O$, $FeCl_3.6H_2O$ and NaOH as precursor in the presence of inert salt, NaCl. Equation 3.1 shown below gives the chemical reaction related to cobalt ferrite preparation.

$$CoCl_2.\ 6H_2O + 2FeCl_3.6H_2O + 8NaOH + n\text{NaCl} \rightarrow CoFe_2O_4 + (n + 8)\text{NaCl} + 22H_2O \quad \text{(Eq.3.1)}$$

FE-SEM was utilized in order to reveal the morphological properties of $CoFe_2O_4$ magnetic nanoparticles. The result is given in Figure 3.1. According to given figure the size of the $CoFe_2O_4$ nanoparticles lay between 10 to15 nm.

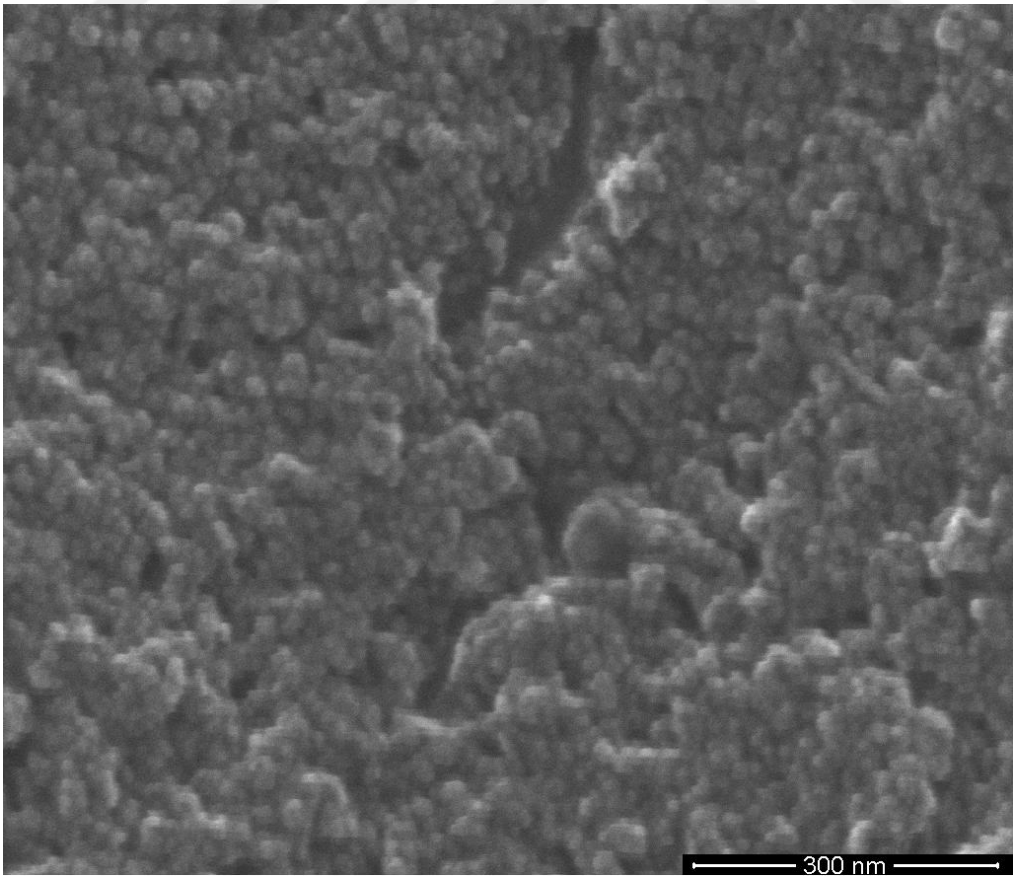

Figure 3.1 FE-SEM image of $CoFe_2O_4$ magnetic nanoparticles.

The elemental composition of the $CoFe_2O_4$ magnetic nanoparticles was determined by EDX measurement coupled with FE-SEM. Figure 3.2 shows the obtained EDX pattern. The EDX pattern confirms the presence of metals added to the structure in the preparation part.

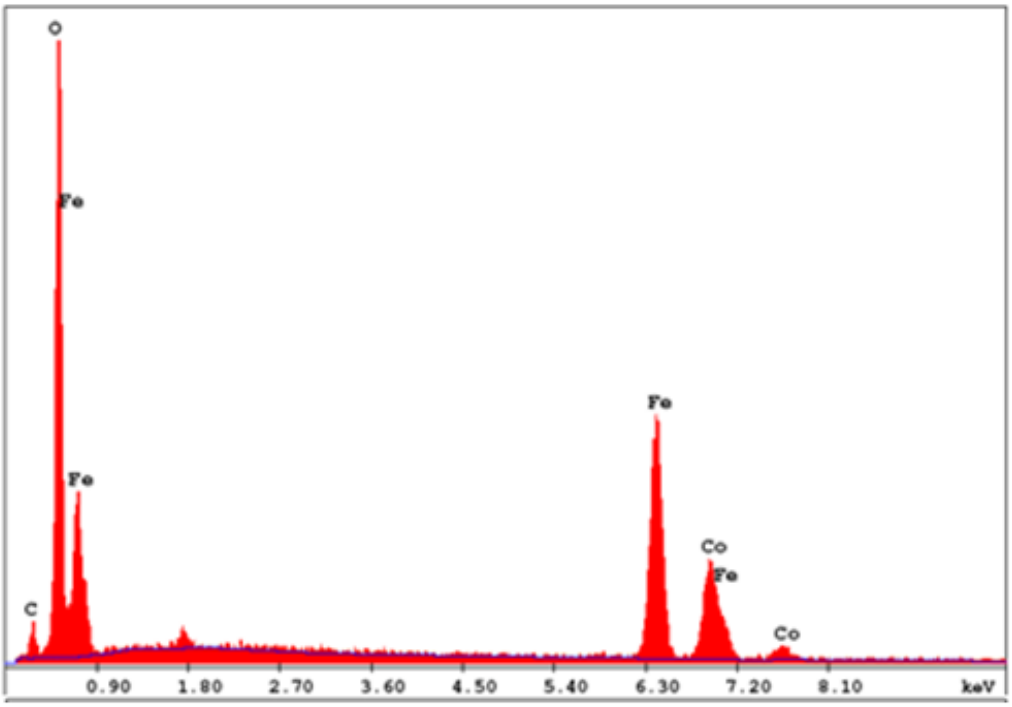

Figure 3.2 EDX pattern of $CoFe_2O_4$ magnetic nanoparticles.

DLS (zeta sizer) was used to figure out the particle size distribution of prepared $CoFe_2O_4$ nanoparticle agglomerates. Figure 3.3. shows the histogram obtained at the end of the measurement. According to DLS (zeta sizer) results and obtained histogram, the zeta average mean size of the $CoFe_2O_4$ agglomerates at pH ~7 was founded as 127.4 nm. The particle size distribution of the $CoFe_2O_4$ nanoparticle agglomerates was in the range of 50 and 220 nm which is compatible with the FE-SEM image.

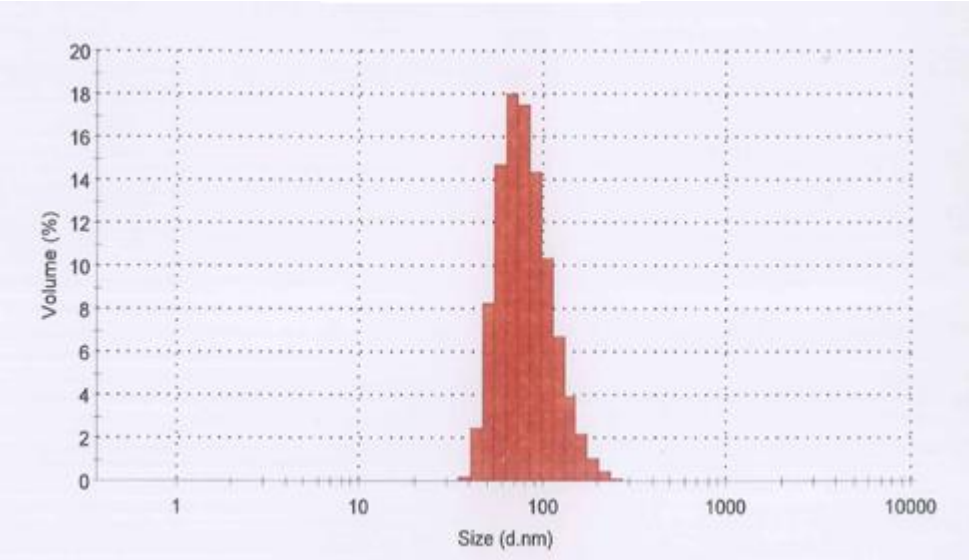

Figure 3.3 A size distribution histogram of $CoFe_2O_4$ magnetic nanoparticles.

3.2. Silica Coating of Cobalt Ferrite (SiO_2-$CoFe_2O_4$) Magnetic Nanoparticles

Silica coating was performed over $CoFe_2O_4$ magnetic nanoparticles to prevent the attraction with the other particles which results agglomeration and to in bigger particle size and provides the surface for addition of nickel and palladium nanoparticles as a host material. The silica coating of magnetic $CoFe_2O_4$ nanoparticles were performed by using Stöber method explained in details in Experimental part.

To figure out the morphology of the cobalt ferrite magnetic core, silica shell (SiO_2-$CoFe_2O_4$) nanoparticles TEM measurement was performed. The obtained image was given in Figure 3.4. It can be clearly seen from Figure 3.4 that the size of SiO_2-$CoFe_2O_4$ aggregates is about 150 nm. Besides, the TEM images showed that the size of the SiO_2-$CoFe_2O_4$ is about 14-20 nm.

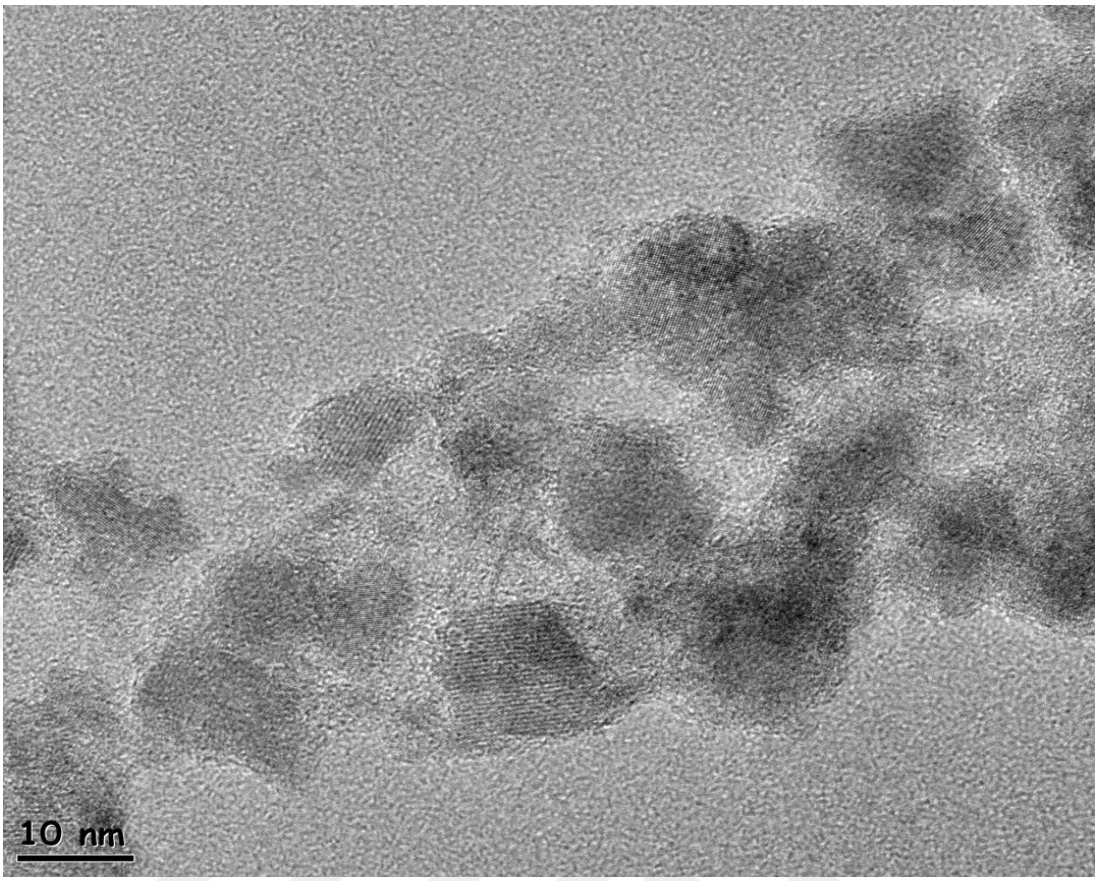

Figure 3.4 TEM image of SiO_2-$CoFe_2O_4$ magnetic nanoparticles.

DLS (zeta sizer) was used to figure out the particle size distribution of prepared SiO_2-$CoFe_2O_4$ nanoparticle agglomerates. Figure 3.5. shows the histogram obtained at the end of the measurement. Size distribution of the agglomerates was founded in the range of 141 and 712 nm from the histogram. The number-length mean size of the prepared SiO_2-$CoFe_2O_4$ nanoparticles was founded as 18 nm from the DLS (zeta sizer) results. These results are compatible with the TEM measurements.

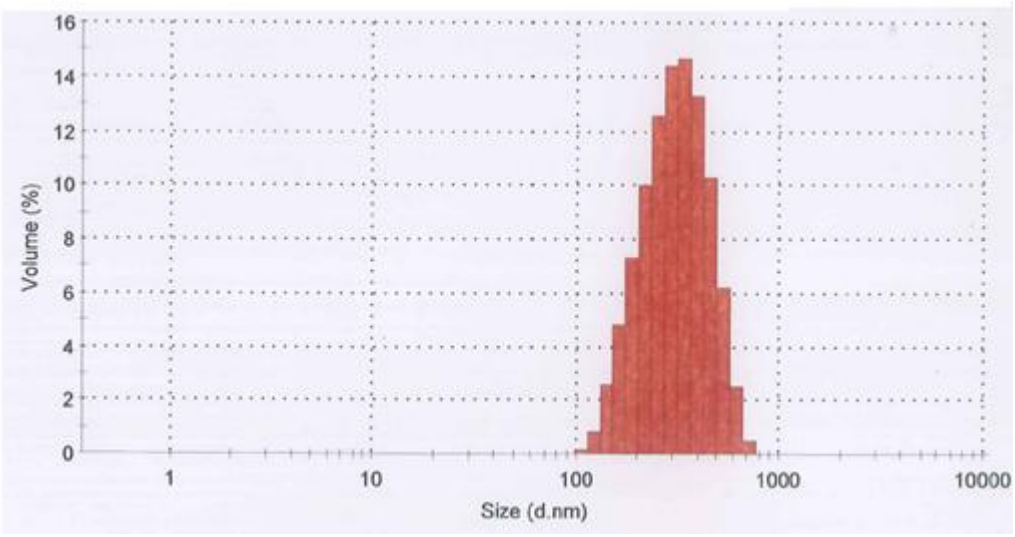

Figure 3.5 A histogram of SiO_2-$CoFe_2O_4$ agglomerates.

The addition of silica shell over $CoFe_2O_4$ magnetic nanoparticles was pointed by EDX analysis. Figure 3.6 shows the EDX patterns of SiO_2-$CoFe_2O_4$ nanoparticles. The EDX pattern confirmed the presence of the silica shell over the $CoFe_2O_4$ magnetic nanoparticles.

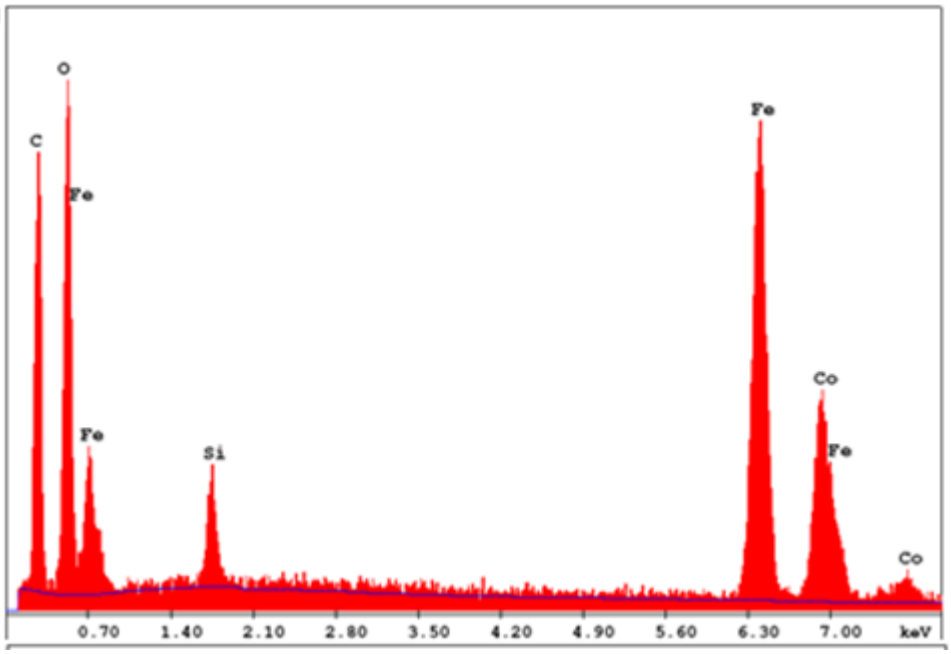

Figure 3.6 EDX patterns of SiO_2-$CoFe_2O_4$ magnetic nanoparticles.

3.2.1. Magnetic Property of Prepared Silica Coated Cobalt Ferrite Nanoparticles

The magnetic behavior of SiO_2-$CoFe_2O_4$ nanoparticles was simply tested by using external magnet. Collection time was checked by putting the prepared particles near the external magnet (Figure 3.7). The total time required to collect particles was recorded as 15 seconds.

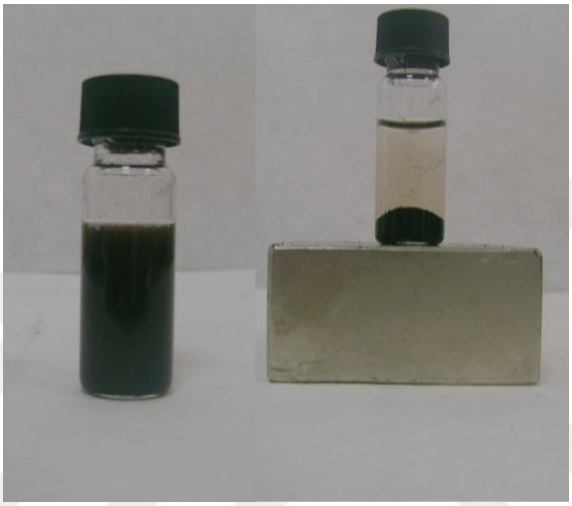

Figure 3.7 Magnetic behavior of SiO_2-$CoFe_2O_4$ after placing near the external magnet which has 1.6 T magnetic field.

Vibrating sample magnetometer (VSM) was used to investigate the magnetic property of the prepared SiO_2-$CoFe_2O_4$ nanoparticles. The saturation magnetization value of prepared SiO2-CoFe2O4 magnetic nanoparticles was measured as 48.0 emu/g. Besides the coercivity (H_c) value was founded as 149.2 Oe.

3.2.2. Surface Area Measurement of Silica Coated Cobalt Ferrite Nanoparticles

BET (Brunauer–Emmett–Teller) measurement was performed to find the surface area and the pore volume of the prepared SiO_2-$CoFe_2O_4$ magnetic nanoparticles. At the end of the measurement, surface area and the pore volume of the support material was found to be 172 m^2/g and 0.8 cm^3/g, respectively.

3.3. Preparation and Characterization of Palladium-Nickel Nanoparticles Supported on Magnetic Platform ($Pd(0)Ni(0)/SiO_2$-$CoFe_2O_4$)

Pd^{2+} and Ni^{2+} ions were added onto SiO_2-$CoFe_2O_4$ magnetic support to prepare $Pd(0)Ni(0)/SiO_2$-$CoFe_2O_4$ catalytic material, by using wet-impregnation method. Then reduction of Pd^{2+} and Ni^{2+} ions were performed on the surface of SiO_2-$CoFe_2O_4$ nanoparticles in aqueous solution during the hydrogen production from NH_3BH_3 at 25.0 ± 0.1 ºC. After the addition of NH_3BH_3 into the solution which containing $Pd(II)Ni(II)/SiO_2$-$CoFe_2O_4$ nanoparticles suspension, reduction of palladium and nickel and hydrogen release occur at the same time. The prepared $Pd(0)Ni(0)/SiO_2$-$CoFe_2O_4$ nanoparticles were isolated from the reaction medium by using external magnet. The characterization of prepared catalyst were performed by using XRD, TEM, SEM, EDX, ICP-OES, XPS and BET techniques.

In order to show the stability of the prepared SiO_2-$CoFe_2O_4$ magnetic support material, XRD measurements of SiO_2-$CoFe_2O_4$ and $Pd(0)Ni(0)/SiO_2$-$CoFe_2O_4$ isolated at the end of the first and fifth run in hydrogen production from NH_3BH_3 were performed. The results are given in Figure 3.8.

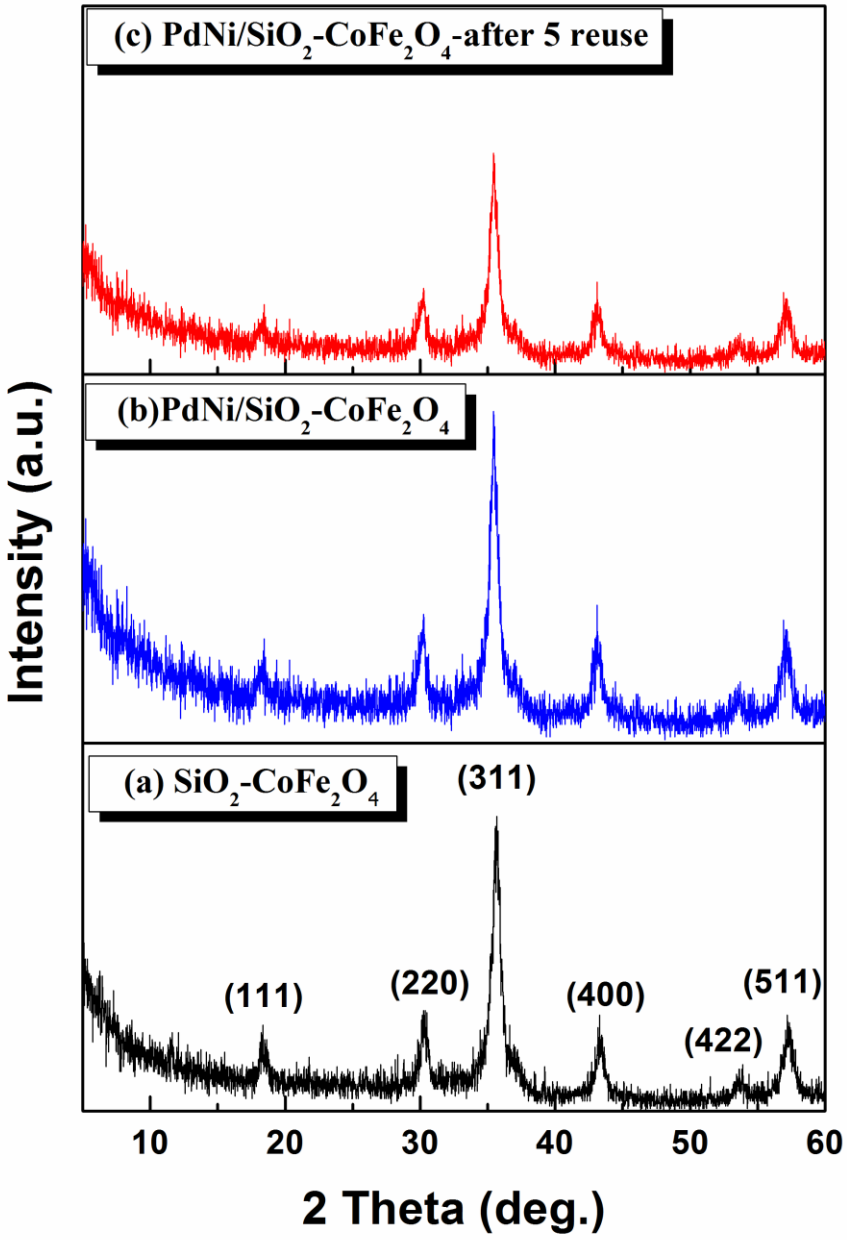

Figure 3.8 XRD patterns of (a) SiO_2-$CoFe_2O_4$, (b) Pd(0)Ni(0)/SiO_2-$CoFe_2O_4$ obtained after the hydrogen production from NH_3BH_3 and (c) Pd(0)Ni(0) /SiO_2-$CoFe_2O_4$ after 5 reuse.

Obtained XRD patterns of SiO_2-$CoFe_2O_4$ and Pd(0)Ni(0)/SiO_2-$CoFe_2O_4$ are given in Figures 3.9(a), (b) and (c) for comparison. Bragg reflections in the 2θ range of 5-60˚ shown in XRD pattern given in Figure 3.9(a) for SiO_2-$CoFe_2O_4$ magnetic support assigned to cubic spinel structure of $CoFe_2O_4$ given in PDF Card 22-1086.

From the same XRD pattern, it can be concluded that the silica shell part is amorphous and the crystallinity of the magnetic $CoFe_2O_4$ nanoparticle (core part) is retained after the addition of silica shell. Figure 3.9(b) and (c) shows the XRD pattern of the Pd(0)Ni(0)/SiO_2-$CoFe_2O_4$ catalyst isolated at the end of the first and fifth run. A comparison of the XRD patterns of Pd(0)Ni(0)/SiO_2-$CoFe_2O_4$ (Figure 3.9(b) and (c)) with SiO_2-$CoFe_2O_4$ (Figure 3.9(a)) clearly showed that the addition of palladium(0) and nickel(0) nanoparticles onto SiO_2-$CoFe_2O_4$ magnetic support caused no observable lost in the crystallinity support material.

The morphology and composition of Pd(0)Ni(0)/SiO_2-$CoFe_2O_4$ were investigated by TEM, EDX coupled with TEM and ICP-OES analyses. Figure 3.9 shows the TEM images of Pd(0)Ni(0)/SiO_2-$CoFe_2O_4$ taken with different magnifications. The size of the PdNi bimetallic nanoparticles was laid between 2-8 nm. As a conclusion, addition of palladium(II) and nickel(II) ions and their reduction to palladium(0) and nickel(0) nanoparticles during the hydrolysis of NH_3BH_3 did not change the structure of the SiO_2-$CoFe_2O_4$ magnetic support, which is in conformance with the XRD results.

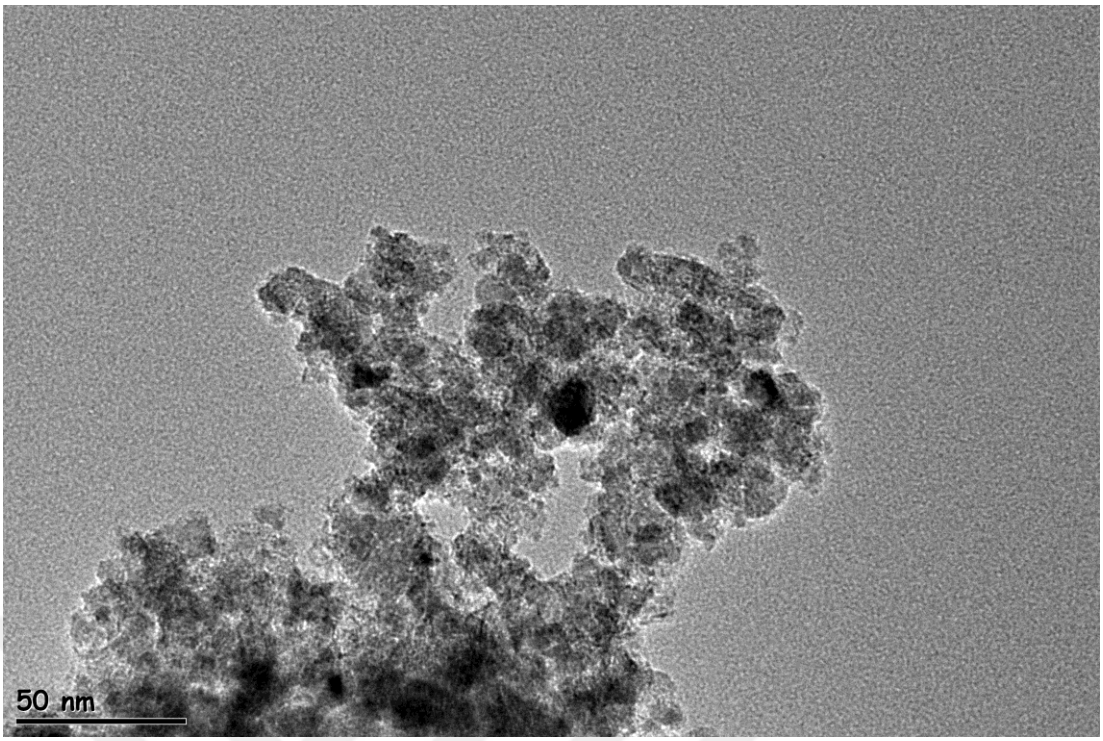

Figure 3.9 TEM image of Pd(0)Ni(0)/SiO_2-$CoFe_2O_4$ nanoparticles.

Palladium and nickel loading of Pd(0)Ni(0)/SiO_2-$CoFe_2O_4$ was revealed by using ICP-OES. According to ICP-OES measurements, the % wt loading of palladium and nickel was 0.45 % and 0.71%, respectively.

The addition of Pd and Ni on to the magnetic support was revealed by EDX besides ICP-OES measurement. Elemental composition of prepared Pd(0)Ni(0)/SiO_2-$CoFe_2O_4$ nanoparticles checked and the result is given in Figure 3.12. EDX patterns of Pd(0)Ni(0)/SiO_2-$CoFe_2O_4$ nanoparticles shows the addition of palladium and nickel onto the magnetic support, SiO_2-$CoFe_2O_4$ magnetic nanoparticles.

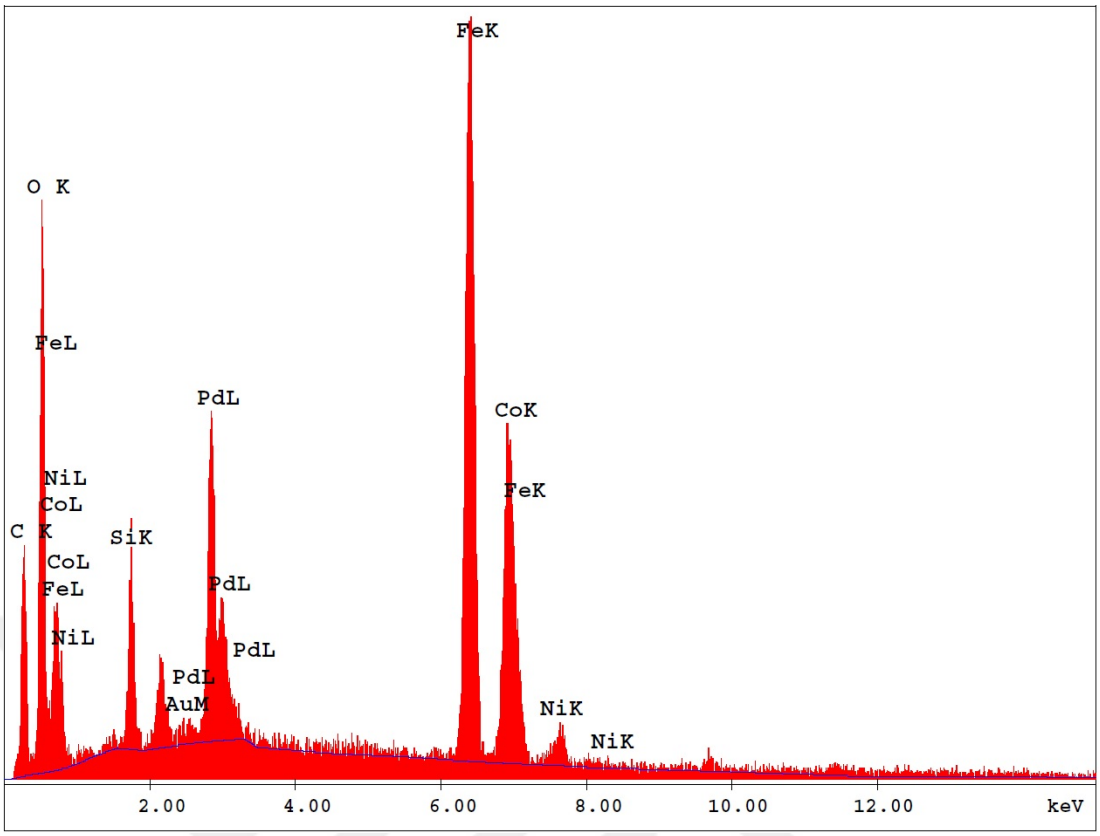

Figure 3.10 EDX patterns of Pd(0)Ni(0)/SiO_2-$CoFe_2O_4$ nanoparticles.

BET (Brunauer–Emmett–Teller) measurement was performed to find the change in surface area and total pore volume of SiO_2-$CoFe_2O_4$ magnetic nanoparticles after addition of Pd and Ni nanoparticles. The surface area and pore volume of the support material was decreased from 172 to 164 m^2/g and from 0.8 to 0.63 cm^3/g respectively. This can be attributed to addition of palladium and nickel nanoparticles onto the surface of SiO_2-$CoFe_2O_4$ magnetic support and formation of Pd(0)Ni(0)/SiO_2-$CoFe_2O_4$ nanostructures.

3.4. Catalytic Activity of Pd(0)Ni(0)/SiO_2-$CoFe_2O_4$ Catalyst

Initially the activity of SiO_2-$CoFe_2O_4$ at different temperature (20, 25, 30, 35 ± 0.1 °C) was checked to see the effect on the hydrolysis of NH_3BH_3. It was found that the magnetic support material (SiO_2-$CoFe_2O_4$) has no catalytic activity in the hydrogen production from NH_3BH_3.

After that the catalytic activities of prepared Pd(0)Ni(0)/SiO_2-$CoFe_2O_4$ catalyst were checked at 25 °C and high activity was obtained in the hydrolysis of NH_3BH_3. Ammonia liberation was also checked and no ammonia liberation was observed during the hydrolysis of NH_3BH_3 by using Pd(0)Ni(0)/SiO_2-$CoFe_2O_4$ catalyst.

After that the effect of % loading of metal on the catalytic activity of Pd(0)Ni(0)/SiO_2-$CoFe_2O_4$ was figured out. For this, a series of loading was checked in the hydrolysis of NH_3BH_3. The results are given in Figure 3.14.

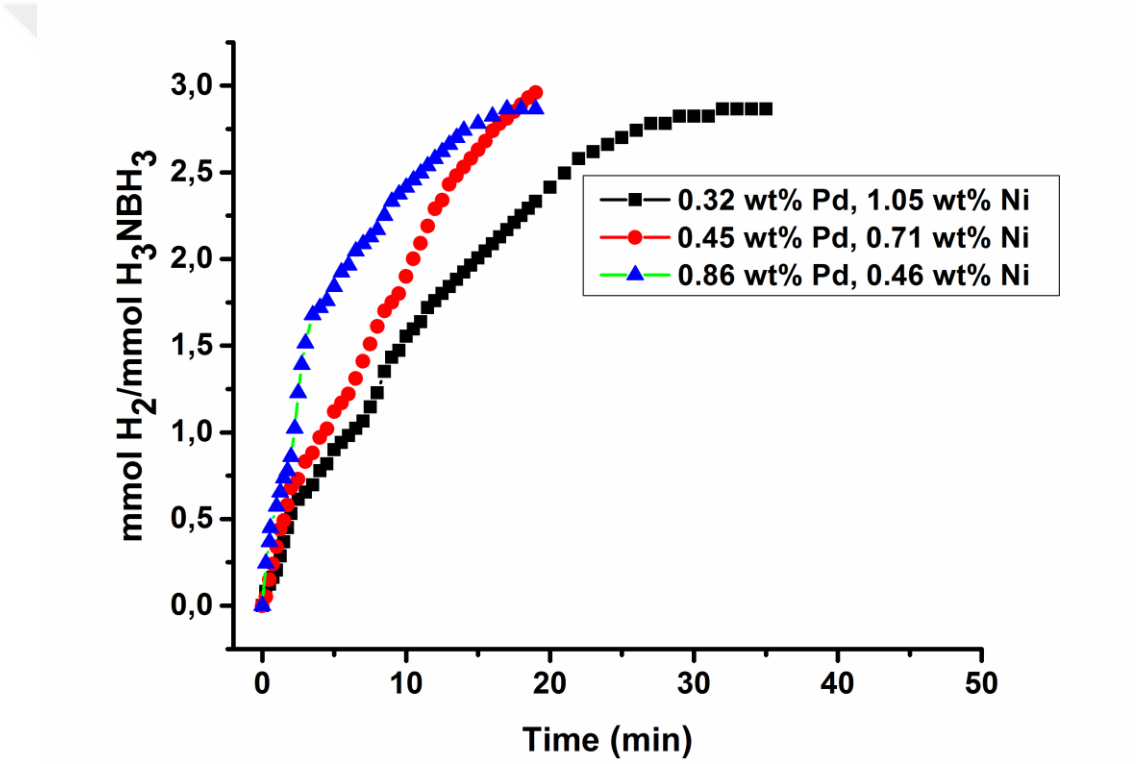

Figure 3.11 Effect of % palladium and nickel loading in Pd(0)Ni(0)/SiO_2–$CoFe_2O_4$ on hydrogen production from NH_3BH_3. (10 mg Pd(0)Ni(0)/SiO_2–$CoFe_2O_4$ catalyst, 100 mM NH_3BH_3 at 25.0 ± 0.1◦C.)

The initial turn over frequencies (TOF) values are given in Table 3.1. According to results given in Table 1, the Pd(0)Ni(0)/SiO_2-$CoFe_2O_4$ catalyst with palladium and nickel loading of 0.45 wt % Pd and 0.71 wt % Ni shows the highest catalytic activity and was chosen and used through the study.

Table 3.1 TOF values for different % metal loadings.

Sample	TOF ((mol H_2/ mol PdNi)×min^{-1})
0.32 wt% Pd, 1.05 wt% Ni	158
0.45 wt% Pd, 0.71 wt% Ni	197
0.86 wt% Pd, 0.46 wt% Ni	174

The TOF value was calculated as 197 (mol H_2/ mol PdNi.min) in the hydrogen production from NH_3BH_3 at 25.0 ± 0.1 °C from the plots given in Figure 3.11 obtained with hydrolysis of 100 mM NH_3BH_3 by using 0.45 wt % Pd and 0.71 wt % Ni SiO_2-$CoFe_2O_4$ magnetic support.

The TOF of the catalyst prepared with palladium and first row metals used in the hydrogen production from NH_3BH_3 are given in Table 3.2 and Table 3.3 in order to make comparison respectively with prepared Pd(0)Ni(0)/SiO_2-$CoFe_2O_4$ catalyst.

Table 3.2 TOF values of palladium based catalysts reported in the literature for the hydrogen production from NH_3BH_3.

Entry	Catalyst	TOF (min^{-1})	Ref.
1	Pd(0)Ni(0)/ SiO_2-$CoFe_2O_4$	197	This study
2	Pd-Co/graphene	37.5	[43]
3	$Co_{0.35}Pd_{0.65}$/C annealed	35.7	[44]
4	Pd/RGO	26.3	[45]
5	$Co_{0.35}Pd_{0.65}$/C	22.7	[44]
6	Pd(0)/SiO_2-$CoFe_2O_4$	254	[46]
7	Pd(0)/HAP	8.3	[47]
8	Pd/zeolite	6.25	[48]
9	Pd/RGO	6.25	[49]
10	Pd/PSSA-co-MA	5	[50]
11	Pd/γ-Al_2O_3	1.39	[51]
12	Pd/C black	0.67	[51]

Table 3.3 TOF values of first row metals based catalysts reported in the literature for the hydrogen production from NH_3BH_3.

Entry	Catalyst	TOF (min^{-1})	Ref.
1	Fe NPs	5	[52]
2	Co/Al_2O_3	2	[53]
3	Ni/Al_2O_3	2	[53]
4	Co NPs	38	[54]
5	Co/Zeolite	4	[55]
6	Ni NPs	5	[56]
7	Ni NPs	1	[57]
8	Ni NPs	9	[58]
9	Ni/Zeolite	5	[59]
10	Cu/Cu_2O	0.3	[60]
11	Cu/Zeolite	0.8	[61]
12	Cu/Co_3O_4	18	[62]
13	$CuNPs/SiO_2$-$CoFe_2O_4$	40	[63]
14	$PdNiNPs/SiO_2$-$CoFe_2O_4$	197	This Study

[a] TOF = mol H_2 / mol metal×min ; [b]

The optimum amount of catalyst was founded by checking the effect of different catalyst concentrations on hydrogen production from NH_3BH_3 were measured. Results are given in Figure 3.15.

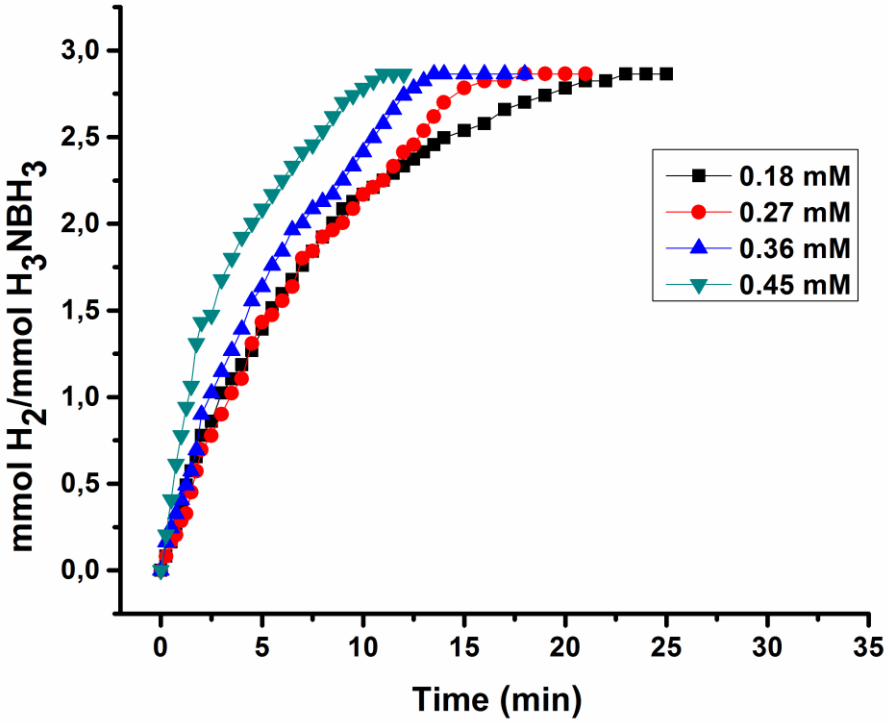

Figure 3.12 Effect of concentration of palladium and nickel founded in Pd(0)Ni(0)/SiO_2–$CoFe_2O_4$ catalyst on hydrogen production from NH_3BH_3. (10 mg Pd(0)Ni(0)/SiO_2–$CoFe_2O_4$ catalyst, 100 mM NH_3BH_3 at 25.0 ± 0.1◦C.)

The calculated TOF numbers from Figure 3.12 are given in table 3.4. The highest activity was observed by using 10 mg (0.18mM) Pd(0)Ni(0)/SiO_2-$CoFe_2O_4$ with a loading of 0.4 wt % Pd and 0.9 wt % Ni respectively.

Table 3.4 TOF values of the prepared catalyst at different concentrations.

Sample [mM]	TOF
0.18	197
0.27	159
0.36	119
0.45	148

The rate constants of hydrogen generation from the hydrogen production from NH_3BH_3 were measured from the linear portions of the plots given in Figure 3.13(a) at five different temperatures in the range of 20-35 °C. Activation energy (E_a) of the reaction catalyzed by Pd(0)Ni(0)/SiO_2-$CoFe_2O_4$ was founded as 53.6 kj/mol from the slope of Arrhenius plot, lnk versus 1/T (K^{-1}) shown in Figure 3.13(b).

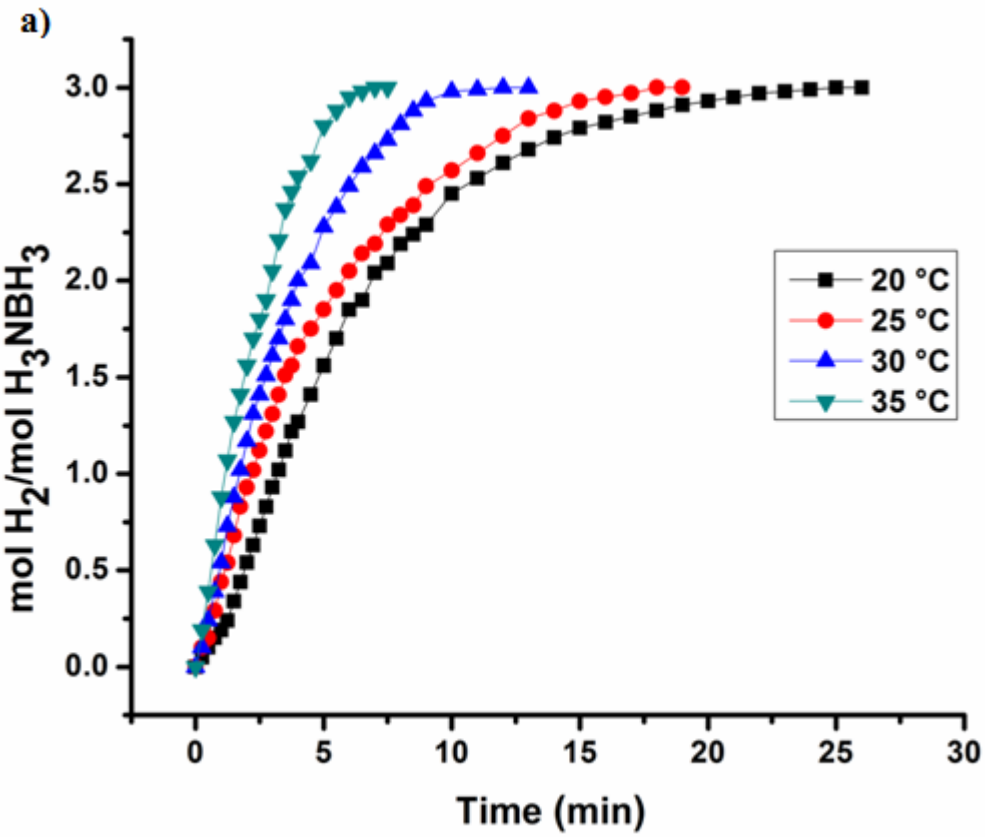

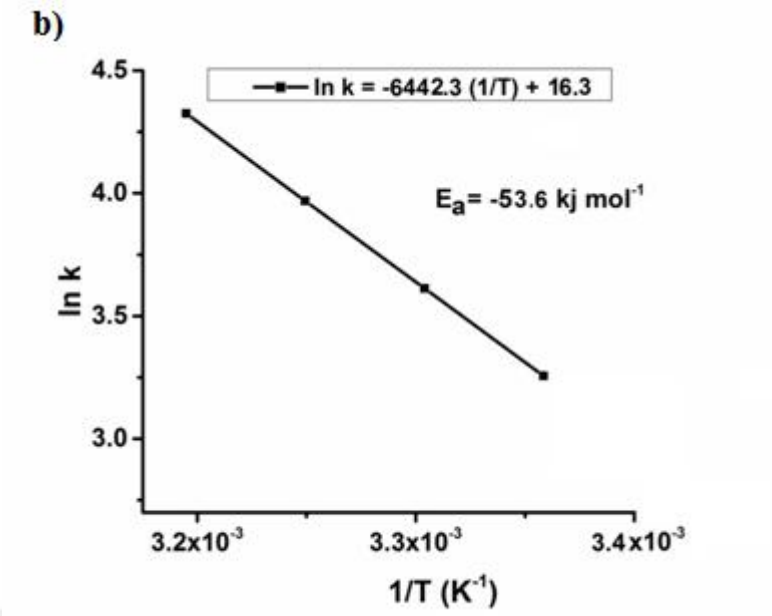

Figure 3.13 (a) Effect of reaction temperature on hydrogen production from NH3BH3. (10 mg Pd(0)Ni(0)/SiO_2–$CoFe_2O_4$ catalyst, 100 mM NH_3BH_3 at 20, 25, 30, 35 ± 0.1◦C.) (b) The Arrhenius plot for the Pd(0)Ni(0)/SiO_2-$CoFe_2O_4$ catalyst.

3.5.The Reuse Performance of Pd(0)Ni(0)/SiO_2-$CoFe_2O_4$ Catalyst

Reuse capacity and easy separation provided by the magnetic support (SiO_2-$CoFe_2O_4$) are the most important properties of Pd(0)Ni(0)/SiO_2-$CoFe_2O_4$ catalyst besides its high catalytic activity. Because it is possible to separate the Pd(0)Ni(0)/SiO_2-$CoFe_2O_4$ catalyst from the reaction solution within seconds by just putting the external magnet near the reaction vessel. After washing the isolated particles in reaction vessel, Pd(0)Ni(0)/SiO_2-$CoFe_2O_4$ catalyst was re-dispersed in a solution containing 100 mM NH_3BH_3. After that, the catalytic activity of the catalyst in the second run of hydrolysis of NH_3BH_3 was checked. To find the reuse capacity hydrogen production from NH_3BH_3 was repeated five times. The results are given in Figure 3.14.

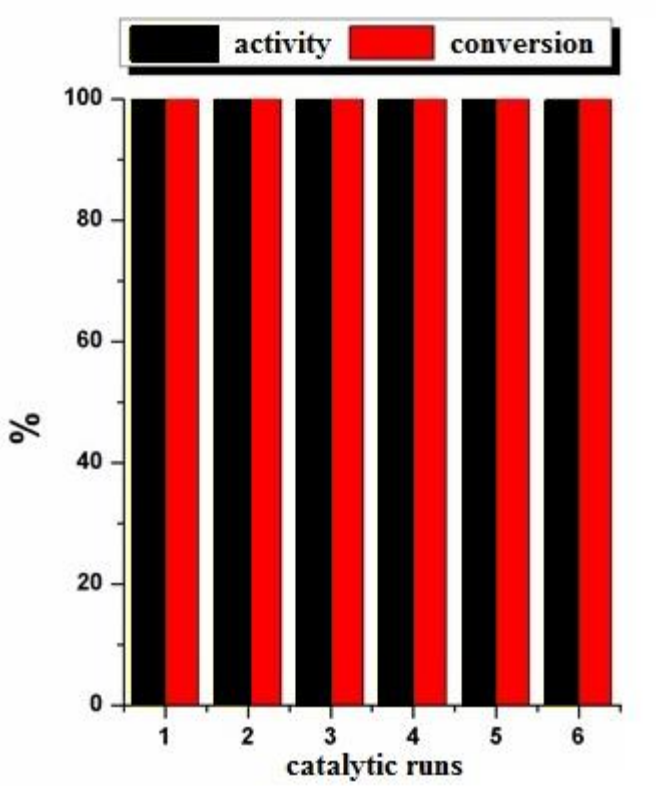

Figure 3.14 Reuse performance of Pd(0)Ni(0)/SiO_2-$CoFe_2O_4$ catalyst in the successive catalytic runs.

According to results given in Figure 3.14 no changes in catalytic activity of Pd(0)Ni(0)/SiO_2-$CoFe_2O_4$ catalyst in the hydrogen production from NH_3BH_3 was observed. The Pd(0)Ni(0)/SiO_2-$CoFe_2O_4$ catalyst retain almost their initial activity after the fifth run with 100% conversion. At the end of the fifth run the solution part was tested by using ICP-OES to see the leaching of Pd and Ni into the solution. According to results, no Pd and Ni ion was founded in the solution at the end of the 5 successive run.

CHAPTER 4

CONCLUSION

As a conclusion, Pd(0)Ni(0)/SiO_2-$CoFe_2O_4$ catalyst with magnetic property can be prepared by adding Pd(II) and Ni(II) ions with wet-impregnation method which is followed by successive reduction of the Pd(II) and Ni(II) ions and production of hydrogen with NH_3BH_3 on the surface of SiO_2-$CoFe_2O_4$ magnetic particles with high activity and reuse capacity. The TOF value of the reaction performed with the Pd(0)Ni(0)/SiO_2-$CoFe_2O_4$ catalyst which are loaded with 0.45 wt % Pd 0.71 wt % Ni was calculated as 197 min^{-1} at 25.0 ± 0.1 ºC.

The Ea (activation energy) of the reaction in which Pd(0)Ni(0)/SiO_2-$CoFe_2O_4$ used was found as 53.6 kJ/mol. Besides the high catalytic activity and low activation energy, it is possible to collect the Pd(0)Ni(0)/SiO_2-$CoFe_2O_4$ catalyst from the solution by using external magnet without taking it to the outside of the reactor, which decreases the total time needed for next run. The reuse performance of the prepared catalyst was checked by using same potion of Pd(0)Ni(0)/SiO_2-$CoFe_2O_4$ catalyst in five successive reactions. Same activity was observed at every run with a complete release of hydrogen.

REFERENCES

1. Siblerud, R. 2001. Our Future is Hydrogen: Energy, Environment, and Economy, New Science Publications: Wellington

2. Satyapala, S., Petrovic, J., Read, C., Thomas, G., Ordaz, G. 2007. Catal. Tod., 120, 246.

3. Staubitz, A., Robertson, A., Manners, I. 2010. Chem. Rev., 110, 4079.

4. Gutowska, A., Li, L., Shin, Y., Wang, C. M., Li, X. S., Linehan, J. C., Smith, R. S., Kay, B. D., Schmid, B., Shaw, W., Gutowski, M., Autrey, T. 2005. Angew. Chem., Int. Ed., 44, 3578.

5. (a) Douglas, T. M., Chaplin, A. B., Weller, A. S. 2008. J. Am. Chem. Soc. 130, 14432, (b) Staubitz, A., Soto, A. P., Manners, I. 2008. Angew. Chem. Int. Ed. 47, 6212, (c) Yang, X., Hall, M. B. J. Am. Chem. Soc. 2008. 130, 1798, (d) Staubitz, A., Sloan, M. E., Robertson, A. P. M., Friedrich, A., Schneider, S., Gates, P. J., Gunne, J. S., Manners, I. 2010. J. Am. Chem. Soc., 132, 13332.

6. (a) Jiang, H.-L., Singh, S. K.,Yan, J.-M, Zhang, X.-B., Xu, Q. 2010. ChemSusChem 3, 541, (b) Jiang, H. L., Xu, Q. 2011. Catal. Tod., 170, 56. (c) Umegaki, T., Yan, J.-M., Zhang, X.-B., Shioyama, H., Kuriyama, N., Xu, Q. 2009, Int. J. Hyd. Energ., 34, 2303.

7. (a) Fortman, G. C., Slawin, A. M. Z., Nolan, S. P. 2011. Organometallic*s*, 30, 5487, (b) Ciganda, R., Garralda, M. A., Ibarlucea, L., Pinilla, E., Torres, M. R., 2010. Dalton Trans. 39, 7226, (c) Graham, T. W., Tsang, C.-W., Chen, X., Guo, R., Jia, W., Lu, S.-M., Sui-Seng, C., Ewart, C. B., Lough, A., Amoroso, D., Abdur-Rashid, K. 2010. Angew. Chem. Int. Ed., *49*, 8708.

8. Thomas, J. M., Thomas, W. J. 1997. Principles and Practice of Heteregeneous Catalysis VCH: New York.

9. (a) Chandra, M.; Xu, Q. 2006. J. Power Sources, 156, 190

10. (a) Simagina, V. I., Storozhenko, P. A.; Netskina, O. V., Komova, O. V., Odegova, G. V., Larichev, Y. V., Ishchenko, A. V., Ozerova, A. M. 2008. Catal. Today, 138, 253, (b) Clark, T. J., Whittell, G. R., Manners, I. **2007**. Inorg. Chem., 46, 7522, (c) Zahmakıran, M., Özkar, S. 2009. App. Catal. A: Gen. 363, 53, (d) Fetz, M., Gerber, R., Blacque, O., French, C. M. 2011. Chem. A Eur. J. 17, 4732, (e) Zahmakıran, M., Özkar, S. 2009. App. Catal. B: Env., 89, 104

11. (a) Rakap, M., Özkar, S. 2010. Int. J. Hyd. Energ., 35, 1305, (b) Rakap, M., Kaku, E. E., Özkar, S. 2011. Int. J. Hyd. Energ. 36, 1448, (c) Rakap, M., Özkar, S. 2011. Int. J. Hyd. Energ. 36, 7019.

12. Mohajeri, N., Raissi, A. T., Adebiyi, O. 2007. J. Power Sources, 167, 482.

13. (a) Yan, J. M., Zhang, X. B., Akita, T., Horuta, M., Xu, Q. 2010. J. Am. Chem. Soc., 132, 5326, (b) Aranishi, K., Jiang, H. L., Akita, T., Horuta, M., Xu, Q. 2011. Nano Research, 4, 1233, (c) Jang, H. L., Umegaki, T., Akita, T., Zhang, X. B., Horuta, M., Xu, Q. 2010, Chem. A Eur. J. 16, 3132.

14. Yan, J. M., Zhang, X. B., Han, S., Shioyama, H., Xu, Q. 2008. Angew. Chem. Int. Ed., 47, 2287.

15. (a) Metin, Ö., Dinç, M., Eren, Z. S., Özkar, S. 2011. Int. J. Hydr. Energ., 36, 11528, (b) Umegaki, T., Yon, J. M., Zhang, X. B., Shioyama, H., Xu, Q. 2010. J. Power Sources, 195, 8209, (c) Metin, Ö., Özkar, S. 2011. Int. J. Hydr. Energ., 36, 1424.

16. (a) Yon, J. M., Zhang, X. B., Han, S., Shioyama, H., Xu, Q. 2009. Inorg. Chem. 48, 7389.

17. Kamada, Y., Yano, K., Xu, Q., Fukuzumi, S. 2010. J. Phys. Chem. C, 114, 16456.

18. Energy Information Administration, Annual Energy Outlook 2005 With Projections To 2025, www.eia.doe.gov/oiaf/aeo/pdf/0383(2005).pdf, February, 2005.

19. U. S. Department of Energy, Basic Research Needs For the Hydrogen Economy, Report of the Basic Energy Sciences Workshop on Hydrogen Production, Storage and Use , www.sc.doe.gov/bes/hydrogen.pdf, May 13-15, 2003.

20. Vladimir A . Blagojević, Dejan G . Minić, Jasmina Grbović Novaković and Dragica M. Minic (2012). Hydrogen Economy: Modern Concepts, Challenges and Perspectives, Hydrogen Energy - Challenges and Perspectives, Prof. Dragica Minic (Ed.), ISBN: 978-953-51-0812-2, InTech.

21. (a) Orimo, S., Nakamori, Y., Eliseo, J. R., Züttel, A., Jensen, C.M. 2007. Chem. Rev., 107, 4111, (b) Schlapbach, L., Züttel, A. 2001. Nature, 414, 353.

22. (a) Sandrock, G., Suda, S., Schlapbach, L. 1992. Hydrogen in Intermetallic Compounsd II, Topics in Applied Physics, Springer-Verlag: Berlin.

23. Rosi, N.L., Eckert, J., Eddaoudi, M., Vodak, D.T., Kim, J., O'Keeffe, M. 2003. Science, 300, 1127.

24. Nikitin, A., Ogasawara, H., Mann, D., Denecke, R., Zhang, Z., Dai, H., Cho, K., Nilsson, A. 2005. Phys. Rev. Lett., 95, 225507.

25. Marrero-Alfonso, Y.E., Beard, A.M., Davis, T.A., Matthews, M.A. 2009. Ind. Eng. Chem. Res., 48, 3703.

26.http://www.sigmaaldrich.com/technical-documents/articles/material matters/recent-developments.html.

27. (a) Chen, Y.S., Fulton, J.L., Linehan, Y.C., Autrey, T. 2005. J. Am. Chem. Soc., 127, 3254, (b) Marder, T.B. 2007. Angew. Chem. Int. Ed., 46, 8116.

28. Baitalow, F., Baumann, J., Wolf, G., Jaenicke, K., Leitner, G. 2002. Thermochim. Acta, 391, 159.

29. Bluhm, M.E., Bradley, M.G., Butterick, R., Kusari, U., Sneddon, L.G. 2006. J. Am. Chem. Soc., 128, 7748.

30. Chandra, M., Xu, Q. 2006. J. Power Sources, 156, 190.

31. Jun, Y.-W., Seo, J.-W., Cheon, J. 2008. Acc. Chem. Res., 41, 179-189.

32. Lu, A.-H., Salabas, E., Schüth, F. 2007. Angew. Chem. Int. Ed., 46, 1222.

33. Gubin, S., Koksharov, Y. A., Khomutov, G., Yu., Y. G. 2005. Russ. Chem. Rev., 74, 489.

34. Tartaj, P., Morales, M. P., Veintemillas-Verdaguer, S., Gonzalez-Carreno, T., Serna, C. 2003. J.Phys.D: Appl. Phys., 36, R182.

35. Liz-Marzn, L. M., Giersig, M., Mulvaney, P. 1996. Chem. Commun., 731.

36. (a) Stober, W., Fink, A., Bohn. E. J. 1968. J. Colloid Interface Sci., 26, 62.

37. Lu, Y., Yin Y., Mayers, B. T., Xia, Y. 2002. Nano Lett., 2, 183.

38. Polshettiwar, V., Varma, R. S. 2008. Chem. Soc. Rev. 37, 1546.

39. Wittmann, S., Sheatz, A., Grass, R. N., Stark, W. J., Reiser, O. 2010. Angew. Chem. Int. Ed., 49, 1867.

40. Shylesh, S., Schünemann, V., Thiel, W. R. 2010. Angew. Chem. Int. Ed., 49, 3428.

41. Kaya, M., Zahmakıran, M., Özkar, S., Volkan, M. 2012. ACS Appl Mater Interfaces, 43866.

42. Stöber, W., Fink, A., Bohn, E. 1968. J. Colloid Interface Sci., 26, 62.

43. Wang, J., Qin, Y.L., Liu, X., Zhang, X.B. 2012. J. Mater. Chem. A: Mater. Energy Sustain, 22, 12468.

44. Sun, D., Mazumder, V., Metin, Ö., Sun, S. 2011. ACS Nano, 5, 6458.

45. Kılıc, B., Sencanlı, S., Metin, Ö. 2012. J. Mol. Catal. A: Chem., 361, 104.

46. Akbayrak S., Kaya M., Özkar S., Volkan M. 2014. Applied Catalysis B: Environmental, 147, 387.

47. Rakap, M., Özkar, S. 2011. Int. J. Hydrogen Energy, 36, 7019.

48. Rakap, M., Özkar, S. 2010. Int. J. Hydrogen Energy, 35, 1305.

49. Xi, P., Chen F., Xie, G. Ma C., Liu, H. Shao, C. Wang, J. Xu, Z. Xu, X. Zeng, Z. 2012. Nanoscale4, 5597.

50. Metin, Ö., Sahin, S., Özkar, S. 2009. Int. J. Hydrogen Energy, 34, 6304.

51. Xu, Q., Chandra, M. 2007. J. Alloys Compd., 446, 729.

52. Yan, J. M., Zhang, X. B., Han, S., Shioyama, H., Xu, Q. 2008. Angew. Chem. Int. Ed. 47, 2287.

53. Xu, Q.; Chandra, M. 2006. J. Power Sources, 163, 364.

54. Xu, Q., Shioyama, H., Zhang, X.B., Yan, J.M. 2010.J. Power Sources,195, 1091.

55. Rakap, M., Özkar, S. 2010. Int. J. Hydrogen Energ., 35, 3341.

56. Umegaki, T., Yon, J. M., Zhang, X. B., Shioyama, H., Kuriyama, N., Xu, Q. 2009. Int. J. Hydrogen Energ., 34, 3816.

57. Yon, J. M., Zhang, X.B., Han, S., Shioyama, H., Xu, Q. 2009. Inorg. Chem., 48, 7389.

58. Cao, C. Y., Chen, C. Q., Li, W., Song, W. G., Cai, W. 2010. ChemSusChem., 3, 1241.

59. Zahmakıran, M., Ayvalı, T., Akbayrak, S., Çalışkan, S., Çelik, D., Özkar, S. 2011. Catal. Tod., 170, 76.

60. Jagirdar, B. R., Sanyal, U., Kalindirdi, B. B. 2008. Phys. Chem. Chem. Phys., 10, 5870.

61. Zahmakıran, M., Durap, F., Özkar, S. 2010. Int. J. Hydrogen Energ., 35, 187.

62. Kamada, Y., Yano, K., Xu, Q., Fukuzumi, S. 2010. J. Phys. Chem. C, 114, 16456.

63. Kaya M., Zahmakiran M., Özkar S., Volkan M., ACS Appl. Mater. Interfaces 2012, 4, 3866.